



Cite this: *Mater. Horiz.*, 2022, 9, 835

Received 26th October 2021,  
Accepted 14th December 2021

DOI: 10.1039/d1mh01741a

[rsc.li/materials-horizons](http://rsc.li/materials-horizons)

Direct ink writing (DIW) of Pickering emulsions offers great potential for constructing on-demand objects. However, the rheological properties of fluid emulsions greatly undermines the shape fidelity and structural integrity of 3D-printed structures. We solve here these challenges and realize a new route towards complex constructs for actual deployment. A dynamic, supramolecular host-guest hydrogel based on poly(ethylene glycol) and  $\alpha$ -cyclodextrin was synthesized in the continuous phase of cellulose nanocrystal-stabilized Pickering emulsions. The storage modulus of the obtained emulgels could reach up to  $\sim 113$  kPa, while being shear thinning and yielding precise printability. Diverse complex architectures were possible with high shape fidelity and structural integrity. The printed objects, for example a double-wall cylinder with 75 layers, demonstrated excellent dimensional stability (shrinkage of  $7 \pm 2\%$  after freeze-drying). With the merits of a simple fabrication process and the high biocompatibility of all the components, the concept of dynamic supramolecular hydrogel-reinforced emulgels represent a potentially versatile route to construct new materials and structures *via* DIW for use in bioproducts and biomedical devices.

## 1 Introduction

Three-dimensional (3D) printing technologies opened an avenue for constructing functional materials featuring unusual shapes and exquisite structures in an efficient and cost-effective way. 3D printing approaches to date have been widely used in various

### New concepts

In this manuscript, the concept of dynamic supramolecular hydrogel-reinforced emulgels has been demonstrated to overcome the significant limitations of direct ink writing of Pickering emulsions with undesirable rheological properties. Although various strategies including increasing the internal phase fraction, jamming the particles at the oil/water interface and incorporating viscous components, have been developed to formulate Pickering emulsions into printable inks, combinations of a dynamic supramolecular hydrogel with such multiphase systems have never been reported before. This study highlights the role of a dynamic supramolecular hydrogel in emulgel-based inks for 3D printing. The dynamic host-guest hydrogel constructed in the continuous phase of the emulgels could simultaneously improve the storage moduli and viscosities of the resultant inks and maintain their shear-thinning behavior, thus realizing the 3D printing of complex structures with high shape fidelity and structural integrity. Additionally, the 3D-printed geometries underwent an approximate  $7 \pm 2\%$  volume shrinkage after freeze-drying, demonstrating an outstanding structural retention, the best reported so far. This study will open up new research fields for 3D printing of Pickering emulsions, for instance, designing and synthesizing on-demand dynamic hydrogels to reinforce emulgels for high-quality 3D printing.

fields ranging from aerospace, biomedicine to microelectronics, and many more.<sup>1-3</sup> Among the currently available 3D printing technologies, direct ink writing (DIW) offers the possibility of creating on-demand objects *via* simple extrusion even without extra manufacturing steps, such as thermal curing and photopolymerization.<sup>4</sup> The mild processing conditions combined with a broad range of material compositions suitable for DIW make this technique attractive, particularly in bio-related applications such as cosmetics, food, pharmaceuticals, sensors, or scaffolds for tissue engineering.

The ability of emulsions to incorporate polar and nonpolar ingredients into their respective hydrophilic and hydrophobic phases, are among the preferred systems for such applications.<sup>5</sup> Over the last decade, emulsions stabilized by solid particles instead of surfactants, Pickering emulsions, have attracted focal attention owing to their multiple advantages

<sup>a</sup> Department of Colloid Chemistry, Max Planck Institute of Colloids and Interfaces, Potsdam 14476, Germany. E-mail: svitlana.filonenko@mpikg.mpg.de

<sup>b</sup> Department of Bioproducts and Biosystems, School of Chemical Engineering, Aalto University, Vuorimiehentie 1, Espoo, FI-00076, Finland

<sup>c</sup> The Bioproducts Institute, Department of Chemical and Biological Engineering, and Department of Chemistry and Wood Science, University of British Columbia, 2360 East Mall, Vancouver, BC, V6T 1Z4, Canada. E-mail: orlando.rojas@ubc.ca

† Electronic supplementary information (ESI) available. See DOI: 10.1039/d1mh01741a

‡ These authors contributed equally to this work.



such as superior stability and low toxicity.<sup>6</sup> Considering the benefits of DIW and the inherent merits of Pickering emulsions, exciting opportunities emerge for constructing new functional materials, relevant to uses ranging from cosmetics and food to pharmaceuticals and biomedical devices.

The prerequisite for successful DIW is to design suitable inks with well-controlled rheological properties. The inks have to exhibit shear-thinning behavior to allow efficient flow through the deposition nozzle under shear stress, and redevelop a sufficiently high storage modulus directly after printing, for shape retention. Additionally, a homogeneous ink is required to enable consistent printing and prevent nozzle clogging.<sup>7</sup> Despite the fact that Pickering emulsions generally display shear thinning behavior, the low zero shear viscosity and storage modulus in most cases still cannot fulfill the demands for DIW, especially in the manufacture of sophisticated and complex architectures. Moreover, high shape fidelity, high structural integrity and low shrinkage remain the main challenges when using multiphase systems for 3D fabrication. Several strategies have been proposed to enhance the printability of Pickering emulsions. For example, they can be formulated into gel-like inks by increasing the internal phase fraction to higher than 74 vol%.<sup>8</sup> The obtained high internal phase Pickering emulsions (HIPPE) generally possess an improved viscosity and storage modulus, because of the enhanced interactions between the closely packed droplets. Unfortunately, leakage of the dispersed phase generally occurs after drying the printed objects. In addition, the special surface properties of the particles required in HIPPE stabilization greatly limit their broad applicability.<sup>9,10</sup> Recently, Xing *et al.* realized<sup>11</sup> the fabrication of Pickering emulsion gels (emulgels) suitable for DIW *via* jamming nanoparticles at the oil/water interface and in the continuous phase, which required surfactants as coagents. Generally, removing the need for surfactants will reduce the complexity and need for testing their effect on biocompatibility and bioactivity, thus potentially extending the applicability of the products. An alternative approach to achieve the gelation of Pickering emulsions into printable inks for DIW is to incorporate viscous components in the hydrophilic or hydrophobic phases.<sup>12,13</sup> The latter process usually involves the utilization of organic solvents, such as dichloromethane and chloroform, to dissolve the hydrophobic component, which is not desirable for many uses. Therefore, the production of biocompatible emulsion inks with excellent printability for DIW is in our opinion an area that is largely unexplored.

Cyclodextrins (CDs), a set of naturally occurring cyclic oligosaccharides made of six ( $\alpha$ -CD), seven ( $\beta$ -CD) or eight ( $\gamma$ -CD) repeating glucose units, can act as hosts to form inclusion complexes with guest molecules possessing suitable structural and physicochemical properties.<sup>14</sup> Studies have demonstrated that such inclusion complexation of appropriate guest molecules lead to CD-based supramolecular hydrogels.<sup>15,16</sup> Unlike the synthesis of most covalently bonded hydrogels, only mild conditions are required for the construction of CD-based, host-guest supramolecular hydrogels. More importantly, such systems generally display thixotropy as well as reversibility

(aka “self-healing”), which facilitate flow through nozzles.<sup>15</sup> Considering these advantages, we report here a simple and versatile approach to address the above challenges by constructing an  $\alpha$ -CD/polyethylene glycol (PEG) supramolecular hydrogel based on host-guest interactions in the continuous phase of Pickering emulsions stabilized with cellulose nanocrystals (CNC) (Fig. 1a). The dynamic hydrogels derived from all-biocompatible components in the ink (a Pickering emulgel) could simultaneously improve the rheological properties (*e.g.*, viscosity and storage moduli) and remain shear-thinning, enabling high-performance DIW (*e.g.*, low shrinkage, high fidelity and high structural integrity).

## 2 Results and discussion

### 2.1 Preparation and characterization of pickering emulgel-based inks

Cellulose nanocrystals (CNCs) are biobased, biocompatible nanoparticles that can assemble at oil/water interfaces and act as efficient stabilizers.<sup>17</sup> In this work, rod-like CNCs were prepared by using an ammonia formate/glycolic acid deep eutectic solvent.<sup>18</sup> The isolated CNCs have an average width of 15–20 nm and a length of 150–250 nm, as revealed using TEM (Fig. 1a). It is noteworthy that, unlike CNCs produced using sulfuric acid hydrolysis, ours display a low positive zeta potential value of about +17 mV. Such an electrostatic charge results in weak electrostatic repulsion between the CNCs and thus enables their excellent emulsifying and stabilizing performance in oil-in-water (O/W) emulsions. Gel-like O/W emulsions with different oil (sunflower oil) fractions, ranging from 56% to 82% (see the ESI,† Fig. S1a), were produced using CNCs as the sole stabilizer at low concentration, 0.8 wt% (with respect to the water phase). The resultant emulgels, referred to as “precursor” emulgels, were named “emulgel-X”, where X indicates the internal phase fraction, which was varied from 56, 67, 75 to 82.

It has been shown that inks suitable for DIW must exhibit shear-thinning behavior, allowing efficient flow through fine deposition nozzles and a sufficiently high storage modulus to retain their shape after printing.<sup>19,20</sup> As illustrated in Fig. S1b (see the ESI,†), all the prepared emulgels were shear thinning. Additionally, within the linear viscoelastic region (LVR), the storage modulus ( $G'$ ) of all the emulgels was always higher than the loss modulus ( $G''$ ) (see the ESI,† Fig. S1c). Such characteristics indicated the predominant elastic, gel-like behavior of the emulgels. Note: this can be quickly prescreened by the fact that all the emulgels do not flow in inverted glass bottles (see the ESI,† Fig. S1a). It is noteworthy that, a desirable ink for high-quality DIW was not possible with the precursor CNC-based Pickering emulgels, as predicted from the low storage modulus ( $< 2$  kPa), as measured within the LVR over a frequency range of 0.01 to 100 rad s<sup>-1</sup> (see the ESI,† Fig. S1d). To retain the shape (a diameter of 0.41 mm) and spanning length (0.5–0.35 mm) of the extruded filaments, the storage modulus of the inks should be in the range of 2.5–5 kPa, according to beam theory calculations.<sup>21</sup>



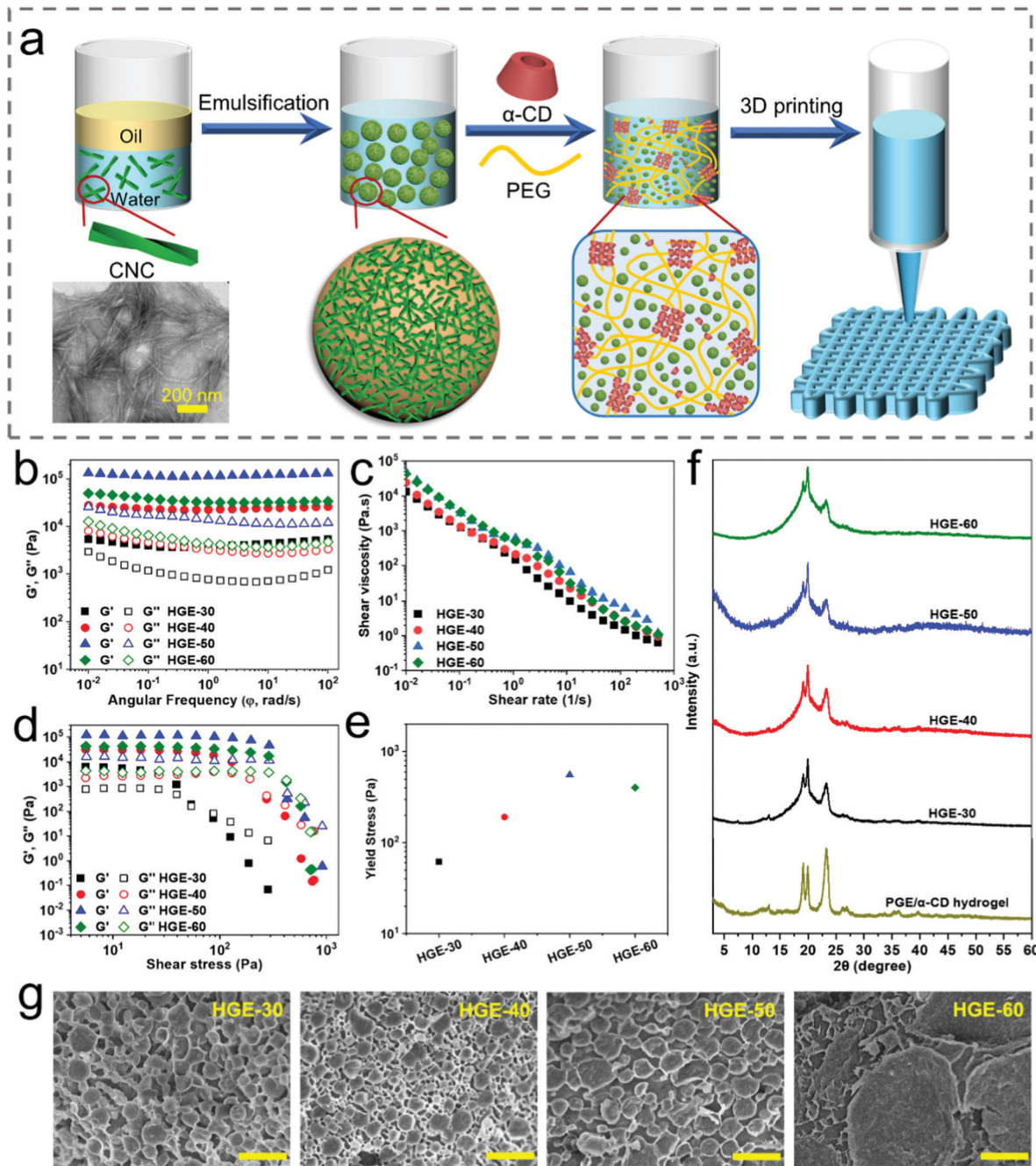


**Fig. 1** (a) Schematic illustration of the fabrication of the emulgels using sunflower oil as the dispersed phase for DIW, including the precursor emulgel (emulgels-*X*) and the host–guest emulgel (HGE-*Y*), where *X* and *Y* refer to the oil fraction. (b) Frequency sweep of the HGEs with different oil phase fractions. (c) Steady state flow curves and (d) stress sweep profiles for the HGEs with different oil phase fractions, as noted. (e) Shear yield stress of the HGE inks. (f) X-Ray diffraction patterns of the HGEs with different oil phase fractions and that of the  $\alpha$ -CD/PEG hydrogel synthesized with a molar ratio of the PEG repeat unit to  $\alpha$ -CD of 30/1. (g) Cryo-scanning electron microscopy (Cryo-SEM) images of the HGEs with different oil phase fractions. Scale bar: 5  $\mu$ m.

To enhance the printability of the systems, a supramolecular hydrogel based on  $\alpha$ -CD/PEG was formed in the continuous phase of the CNC-stabilized emulgels (Fig. 1a). The produced host–guest supramolecular hydrogels are referred to as HGE-*Y*, where *Y* is the oil phase fraction. Similar to the precursor Pickering gels stabilized solely by CNC (in the absence of  $\alpha$ -CD/PEG), all the HGEs displayed a higher storage modulus

than the loss modulus (Fig. 1b), indicating elastic behavior. Compared to the original formulations (emulgel-56, emulgel-67, emulgel-75 and emulgel-82), the storage modulus of the HGEs (HGE-30, HGE-40, HGE-50 and HGE-60) increased by at least one order of magnitude. HGE-30, HGE-40 and HGE-50 exhibited storage moduli of around 5 kPa, 22 kPa and 113 kPa, respectively. The storage modulus of HGE-60 (32 kPa) was lower

than that of HGE-50. Except for HGE-30, all the other HGEs have a sufficiently high storage modulus for printable inks and exceed the theoretical target calculated using the beam theory.<sup>21</sup> Importantly, all the HGEs with high apparent viscosities still exhibited pronounced shear thinning behavior (Fig. 1c). The shear viscosity decreased by several orders of magnitude as the shear rate increased from 0.01 to 500  $1\text{ s}^{-1}$ . All these properties support the preservation of the dynamic nature of the host–guest interactions even in the presence of the Pickering emulsion with possibly competing interactions.  $\alpha$ -CD rings were threaded on the PEG chains, resulting in the formation of  $\alpha$ -CD/PEG poly(pseudo)rotaxanes.<sup>22,23</sup> Unlike the hydrogels formed with irreversible covalent bonds, the supramolecular hydrogels based on non-covalent host–guest interactions generally have dynamic and reversible character. However, this physical crosslinking alone, based on host–guest interactions, only generated hydrogels that were too weak. As shown in Fig. S3 (see the ESI†), the  $\alpha$ -CD/PEG supramolecular hydrogel displayed shear-thinning behavior, but its low storage modulus (see the ESI,† Fig. S4) was not sufficient to support shape retention after printing.

Oscillatory measurements at low strains were also conducted to further assess the rheological properties of the HGEs. All the HGEs exhibited consistent and predominantly elastic behavior ( $G' > G''$ ), which is in line with results revealed by the frequency sweep measurements. HGE-50 had the highest yield stress,  $\tau_y$  ( $G' = G''$ ), although the value is quite low, 556 Pa (Fig. 1e). The low shear yield stress guarantees the smooth flow of the HGEs through the nozzle under the applied nozzle shear stress, but also facilitates a potential application in bio-related sectors. For example, it has been shown that the shear stress applied within the nozzle during the printing process had a decisive impact on cell viability.<sup>24</sup> In this work, Blaeser *et al.* reported that the average cell viability (96% cell viability) was almost unaffected by the printing process when cells were exposed to low shear stress (<5 kPa), while the viability of the cells considerably decreased, to 91% and 76%, for an applied nozzle shear stress of 5–10 kPa and >10 kPa, respectively. Thus, because of the rather ideal rheological properties and the high biocompatibility of all the components, we believe that HGEs would be a promising ink for DIW.

XRD measurements were performed to gain further insight into the local organization of the HGEs. The diffraction patterns of all the HGEs and the  $\alpha$ -CD/PEG hydrogel exhibited reflections at  $2\theta = 13.0^\circ$  and  $19.9^\circ$ , which are the characteristic peaks for the dried-out channel type  $\alpha$ -CD inclusion complexes.<sup>25,26</sup> The strong reflections at  $2\theta$  values of  $19.2^\circ$  and  $23.2^\circ$ , arising from crystalline PEG, were also observed in all the dried samples.<sup>27</sup> Full threading relies on a ratio of the PEG repeat unit to  $\alpha$ -CD of 2.<sup>25</sup> A much higher molar ratio of the PEG repeat unit to  $\alpha$ -CD of 30/1 was employed in this work to synthesize the supramolecular hydrogel, *i.e.*, we observe with the PEG peaks the unthreaded linear connecting chains.

Compared with the precursor emulgels (see the ESI,† Fig. S1a), the HGEs (Fig. 1g and Fig. S2, ESI†) included smaller oil droplets, ranging from several to dozens of microns.

Cryo-SEM images of the HGEs (Fig. 1g) showed that the oil droplets were trapped within a 3D matrix formed by the  $\alpha$ -CD/PEG hydrogel. The barrier layers formed with CNCs around the droplets endowed the emulsions with sufficient mechanical stability, preventing the droplets from transport, collision and rupture within the continuous phase containing the  $\alpha$ -CD/PEG hydrogel. The restricted droplet motion reduces their contact and/or aggregation, leading to the excellent long-term stability of the HGEs. No oil-leakage, creaming nor phase separation were observed in the HGEs using a naked eye inspection, even after storage at room temperature and humidity for more than 6 months.

## 2.2 3D Printing of pickering emulgels

For some biological applications, shape fidelity and structural integrity remarkably affect the overall performance of 3D printed structures. All the HGEs demonstrated excellent flowability under the studied printing conditions (Table S1, ESI†). This was due to their shear-thinning behavior and yield stress, which was lower compared to the stress on the nozzle tip. The HGEs were extruded successfully through nozzles with a diameter as small as 250  $\mu\text{m}$  (25 G). The effect of various nozzle diameters on the quality and the resolution of the printed structures is indicated in Fig. 2a; the theoretical infill density and the infill pattern are the same in all three structures (infill density: 30%, infill pattern: grid-lattice). A higher nozzle gauge (smaller diameter) was attributed to the more significant shear and a decrease in the apparent viscosity when extruding the material, which is a typical behavior in shear-thinning inks. The samples HGE-40, HGE-50, and HGE-60 exhibited excellent

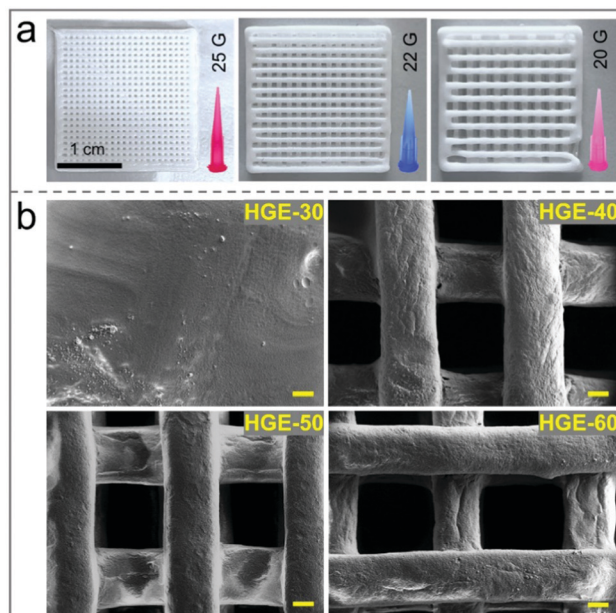
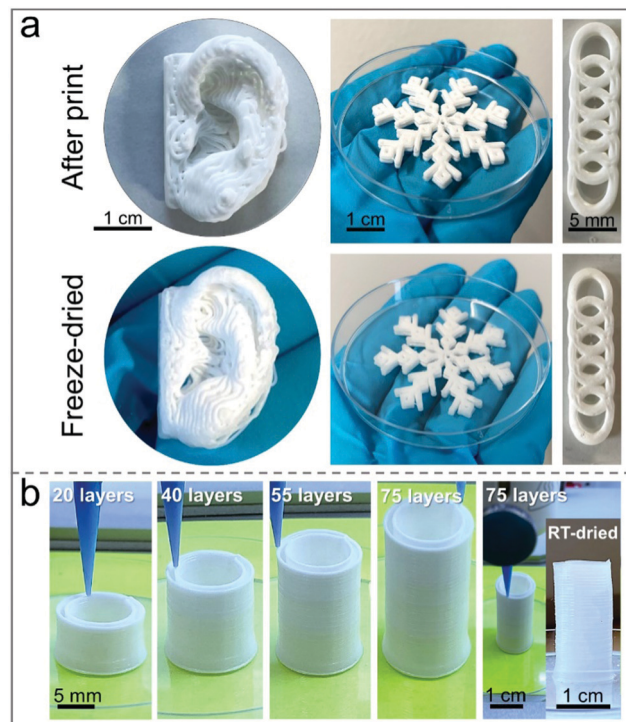


Fig. 2 (a) Top view of cubic grids printed with HGEs-50 using conical bioprinting nozzles red (diameter 250  $\mu\text{m}$ , 25 G), blue (diameter 410  $\mu\text{m}$ , 22 G), and pink (diameter 630  $\mu\text{m}$ , 20 G). (b) SEM images of the cubic grids printed with HGE-30, HGE-40, HGE-50 and HGE-30. The scale bar in all the SEM images is 200  $\mu\text{m}$ .





**Fig. 3** (a) 3D Printed complex structures obtained by DIW of HGE-50 in the shape of a support-free ear, a snowflake, and interconnected circles in a high axial structure before and after freeze-drying. (b) The progression of the structures formed by the deposition of 75 layers (3 ml of HGE-50) after printing and drying at room temperature.

stability, structural fidelity, and distinguishable layers after printing, according to the SEM images in Fig. 2b. As discussed in the rheological characterizations, the lower structural stability of HGE-30 after printing is attributed to the low storage modulus, and merging of the 3D printed filaments/layers is observed, in contrast to the other samples.

The printing quality and the structural integrity of the HGEs were investigated thoroughly by printing more complex structures (Fig. 3 and Fig. S5, ESI†). The HGE-50 reflected the highest print quality when many layers were deposited in a layer-by-layer manner. The 3D-printed geometries underwent an approximate  $7 \pm 2\%$  volume shrinkage after freeze-drying, demonstrating an outstanding structural retention, the best reported so far.<sup>12,28</sup> In addition to the printed letters (see the ESI,† Fig. S5), the high resolution of the printed structures is shown as a support-free 3D-printed ear, a snowflake, and interconnected circles in a cylinder (Fig. 3a). One of the main challenges in DIW is the deposition of many layers due to the low solid content of printing ink that does not facilitate adequate support to maintain the top layers. The desirable rheological properties and the large storage modulus in HGE-50 allowed the deposition of 3 mL of emulgel into a double-wall cylinder with 75 layers (Fig. 3b). The 75-layer 3D printed cylinders exhibited  $9 \pm 1.7\%$  shrinkage after drying at room temperature, which is highly comparable with the reported value after freeze-drying (about  $7 \pm 2\%$ ). It is noteworthy that, no oil leakage was observed for the freeze-dried

structures, which have an oil weight content as high as 89% (with respect to the total weight of the freeze-dried structures). Additionally, the printed structures demonstrated good mechanical strength, as is shown in Fig. S6 (see the ESI†) by the dried cubic grid printed with HGEs-50 that can withstand up to a 500 g weight. With all the components employed for DIW being biocompatible, these structures may find various bio-related applications.

### 3 Conclusion

In summary, we developed a simple and potentially versatile approach to allow the DIW of Pickering emulsions into complex architectures with high shape-fidelity and structural integrity. Dynamic supramolecular hydrogels based on PEG and  $\alpha$ -CD were synthesized within the continuous phase around CNC-stabilized Pickering emulsions *via* host-guest interactions. A high storage modulus, up to 113 kPa, was achieved in such systems. The shear-thinning behavior could be maintained due to the dynamic nature of the hydrogel, thus enabling printing. The 3D-printed geometries underwent an approximate  $7 \pm 2\%$  volume shrinkage after freeze-drying with an outstanding dimensional stability. Benefiting from the merits of low-cost, the simple fabrication process of the emulgel inks and the high biocompatibility of all these components, we believe that this work will pave the way for the construction of new materials and structures *via* the DIW of Pickering emulsions, especially for bio-related applications.

### Conflicts of interest

The authors declare no competing financial interests.

### Acknowledgements

B. P., S. F. and M. A. gratefully acknowledge the Max Planck Society for financial support. B. P. would like to thank Branislav Jeriga for preparing some of the CNC samples. A. R. and O. R. acknowledge funding support by the Academy of Finland's Biofuture 2025 program under project 2228357-4 (3D Manufacturing of Novel Biomaterials). O. J. R. is grateful for the support received from the ERC Advanced Grant Agreement No. 788489 ("BioElCell"), the Canada Excellence Research Chair initiative (CERC-2018-00006), and Canada Foundation for Innovation (Project number 38623). R. A. acknowledges funding from the FinnCERES GoGlobal mobility fund. This work made use of the facilities of Aalto University's Nanomicroscopy Center. Open Access funding provided by the Max Planck Society.

### References

- 1 C. Zhang, M. P. Kremer, A. Seral-Ascaso, S. H. Park, N. McEvoy, B. Anasori, Y. Gogotsi and V. Nicolosi, *Adv. Funct. Mater.*, 2018, **28**, 1705506.
- 2 H. Ceylan, I. C. Yasa, O. Yasa, A. F. Tabak, J. Giltinan and M. Sitti, *ACS Nano*, 2019, **13**, 3353–3362.



- 3 Y. Yang, X. Li, M. Chu, H. Sun, J. Jin, K. Yu, Q. Wang, Q. Zhou and Y. Chen, *Sci. Adv.*, 2019, **5**, eaau9490.
- 4 J. A. Lewis, *Adv. Funct. Mater.*, 2006, **16**, 2193–2204.
- 5 G. W. Lu and P. Gao, *Handbook of non-invasive drug delivery systems*, Elsevier, 2010, pp. 59–94.
- 6 J. Wu and G. H. Ma, *Small*, 2016, **12**, 4633–4648.
- 7 Y. Jiang, Z. Xu, T. Huang, Y. Liu, F. Guo, J. Xi, W. Gao and C. Gao, *Adv. Funct. Mater.*, 2018, **28**, 1707024.
- 8 X. Li, X. Xu, L. Song, A. Bi, C. Wu, Y. Ma, M. Du and B. Zhu, *ACS Appl. Mater. Interfaces*, 2020, **12**, 45493–45503.
- 9 Y. Zhu, S. Huan, L. Bai, A. Ketola, X. Shi, X. Zhang, J. A. Ketoja and O. J. Rojas, *ACS Appl. Mater. Interfaces*, 2020, **12**, 11240–11251.
- 10 B. Pang, H. Zhang, M. Schilling, H. Liu, X. Wang, F. Rehfeldt and K. Zhang, *ACS Sustainable Chem. Eng.*, 2020, **8**, 7371–7379.
- 11 Y. Zhang, G. Zhu, B. Dong, F. Wang, J. Tang, F. J. Stadler, G. Yang, S. Hong and F. Xing, *Nat. Commun.*, 2021, **12**, 111.
- 12 S. Huan, R. Ajdary, L. Bai, V. Klar and O. J. Rojas, *Biomacromolecules*, 2018, **20**, 635–644.
- 13 S. Huan, B. D. Mattos, R. Ajdary, W. Xiang, L. Bai and O. J. Rojas, *Adv. Funct. Mater.*, 2019, **29**, 1902990.
- 14 D. Prochowicz, A. Kornowicz and J. Lewiński, *Chem. Rev.*, 2017, **117**, 13461–13501.
- 15 G. Liu, Q. Yuan, G. Hollett, W. Zhao, Y. Kang and J. Wu, *Polym. Chem.*, 2018, **9**, 3436–3449.
- 16 B. V. Schmidt and C. Barner-Kowollik, *Angew. Chem., Int. Ed.*, 2017, **56**, 8350–8369.
- 17 F. Cherhal, F. Cousin and I. Capron, *Biomacromolecules*, 2016, **17**, 496–502.
- 18 E. E. Jaekel, J. A. Sirviö, M. Antonietti and S. Filonenko, *Green Chem.*, 2021, **23**, 2317–2323.
- 19 L. Li, P. Zhang, Z. Zhang, Q. Lin, Y. Wu, A. Cheng, Y. Lin, C. M. Thompson, R. A. Smaldone and C. Ke, *Angew. Chem.*, 2018, **130**, 5199–5203.
- 20 A. Schwab, R. Levato, M. D'Este, S. Piluso, D. Eglin and J. Malda, *Chem. Rev.*, 2020, **120**, 11028–11055.
- 21 J. E. Smay, J. Cesarano and J. A. Lewis, *Langmuir*, 2002, **18**, 5429–5437.
- 22 J. Li, A. Harada and M. Kamachi, *Polym. J.*, 1994, **26**, 1019–1026.
- 23 K. L. Liu, Z. Zhang and J. Li, *Soft Matter*, 2011, **7**, 11290–11297.
- 24 A. Blaeser, D. F. Duarte Campos, U. Puster, W. Richtering, M. M. Stevens and H. Fischer, *Adv. Healthcare Mater.*, 2016, **5**, 326–333.
- 25 A. Harada, J. Li and M. Kamachi, *Macromolecules*, 1993, **26**, 5698–5703.
- 26 T. Uyar, P. Kingshott and F. Besenbacher, *Angew. Chem., Int. Ed.*, 2008, **47**, 9108–9111.
- 27 R. Bhattacharyya and S. K. Ray, *Chem. Eng. J.*, 2015, **260**, 269–283.
- 28 H. Françon, Z. Wang, A. Marais, K. Mystek, A. Piper, H. Granberg, A. Malti, P. Gatenholm, P. A. Larsson and L. Wågberg, *Adv. Funct. Mater.*, 2020, **30**, 1909383.

